Appl. Phys. B 79, 379–382 (2004)
DOI: 10.1007/s00340-004-1557-8

Applied Physics B
Lasers and Optics

G. MÉCHAIN[1]
A. COUAIRON[2,✉]
Y.-B. ANDRÉ[1]
C. D'AMICO[1]
M. FRANCO[1]
B. PRADE[1]
S. TZORTZAKIS[1]
A. MYSYROWICZ[1]
R. SAUERBREY[3]

Long-range self-channeling of infrared laser pulses in air: a new propagation regime without ionization

[1] Laboratoire d'Optique Appliquée, École Nationale Supérieure des Techniques Avancées – École Polytechnique, CNRS UMR 7639, 91761 Palaiseau Cedex, France
[2] Centre de Physique Théorique, École Polytechnique, CNRS UMR 7644, 91128 Palaiseau Cedex, France
[3] Institut für Optik und Quantenelektronik, Max-Wien-Platz 1, 07743 Jena, Germany

Received: 18 March 2004/Revised version: 28 April 2004
Published online: 23 June 2004 •

ABSTRACT We report long-range self-channeling in air of multiterawatt femtosecond laser pulses with large negative initial chirps. The peak intensity in the light channels is at least one order of magnitude lower than required for multiphoton ionization of air molecules. A detailed comparison is made between experiments and realistic $3+1$-dimensional numerical simulations. It reveals that the mechanism limiting the growth of intensity by filamentation is connected with broken revolution symmetry in the transverse diffraction plane.

PACS 42.65.Sf; 42.25.Bs; 42.65.Jx; 52.38.Hb

Understanding the nonlinear propagation of powerful ultrashort laser pulses in the atmosphere has become important in view of several applications. For instance, remote multicomponent pollutant detection [1–3], lightning protection [4, 5], long-range propagation of light bullets [6] and production of secondary sources rely on femtosecond filamentation [7–13]. This term refers to the self-channeling of femtosecond laser pulses in the form of stable high-intensity light filaments. This phenomenon was discovered in the late 1990s with lasers emitting at infrared (IR) wavelengths [7, 14]. Filaments with diameters around 100 μm and peak intensities below 10^{14} W/cm^2 were observed, sufficient to leave in their wake plasma strings with a density around 10^{16} cm^{-3}.

For many applications, a control of femtosecond filamentation over long distances is crucial. A considerable literature has been devoted to the properties of single light filaments with energies in the range 1–10 mJ. They are typically obtained when subpicosecond pulses at near-IR wavelength, with a peak power slightly above a minimum value $P_{cr} \sim$ 5 GW, are launched in air. Femtosecond filamentation in such a case relies on a competition between well-identified nonlinear effects. The whole beam first undergoes self-focusing until the intensity reaches a sufficiently high value to trigger ionization. Plasma defocusing then stops the collapse that would have occurred in the absence of any saturating mechanism. A plasma string is formed at the beginning of the filamentation process, followed further down by occasional ionization spikes that prevent beam collapse, resulting in a self-guided light pulse over several tens of meters. Characteristics of filaments such as the beam diameter, the self-guided pulse intensity, the time profile or the plasma string density are well reproduced by numerical simulations [8, 15].

The propagation of ultra-short pulses with a higher laser power $P \gg P_{cr}$ is less understood. It has been reported by several groups that the inhomogeneous input beam typically breaks up into several spots during the self-focusing stage. Each filament carries about the same energy as in the case of a single filament. A model has been developed to explain this behavior, although no detailed comparison between numerical and experimental results is yet available. In the model, short-scale multifilamentation occurs, due to unavoidable beam irregularities, giving rise to N filaments, with $N \sim P/P_{cr}$. Collapse of each filament is limited by ionization. Each filament eventually gives back most of its energy through diffraction to a common laser-energy pool [16]. Successive multifilamentary patterns with decreasing numbers of filaments are formed, until the reservoir energy is exhausted. The typical distance over which ionizing filaments subsist is of the order of a hundred meters [17, 18].

This letter reports experimental results concerning the propagation of intense short laser pulses along a horizontal path ranging over long distances $d > 500$ m. We observe stable millimeter-size light channels extending over a range of several km [20]. However, in contrast to the usual filaments obtained with small chirp, we find no evidence of ionization in the channels, showing that another mechanism is limiting their peak intensity. In order to obtain insight into this regularizing mechanism, we have compared the experimental results with realistic numerical results, using a nonlinear propagation code which describes successfully the regime $P \gtrsim P_{cr}$. We find that it is not necessary to add any new saturation mechanism to reproduce the experimental results, provided the full three-dimensional aspect of the beam-intensity profile is correctly taken into account. Numerical simulations performed in an ideal case with the addition of small perturbations reveal a crucial feature for regularizing the light channeling over long distances. Each light channel breaks up and nucleates subchannels which compete for the available laser energy. In the absence of an initial intensity perturbation breaking the axial symmetry, the usual ionization-limited filamentation is recovered.

✉ Fax: +33-1/69333008, E-mail: couairon@cpht.polytechnique.fr

Experiments were performed with a CPA (chirped pulse amplification) multiterawatt laser system, called "teramobile" [21]. It consists of a Ti:S oscillator followed by several stage amplifiers, delivering pulses of 200-mJ energy and a minimum duration of about 100 fs at a repetition rate of 10 Hz. The pulse is stretched in time before amplification to avoid damage in the amplifiers and then is recompressed at the output by a compressor stage consisting of a pair of gratings. This scheme allows us to easily adjust the initial pulse duration before launching the laser pulse in the atmosphere, by imparting a residual linear frequency chirp (either positive or negative) to the emitted pulse. The beam diameter at the output of the compressor is 3.4 cm, with a marked top-hat intensity profile. The laser path propagated 3 m above the ground, during a period of the night when air turbulence was minimal.

Measurements of the beam energy and beam-intensity profile were performed at various locations along the propagation path, up to a distance of 2300 m, for various initial chirps. The beam energy was detected with a calorimeter, over a surface of 15-cm diameter. The intensity distribution in the beam was recorded either by direct single-shot exposure of calibrated photographic plates, or by forming the image of a white diffuser put in the path of the beam. In addition, detection of air ionization was performed using different techniques developed for single filaments: direct electrical conductivity [22, 23], detection of low-frequency radiation from the plasma column [24] or detection of the luminescence from ionized nitrogen molecules [25]. Most experiments were performed with a collimated beam with a 3.4-cm-diameter size. Some experiments were also performed using an expanding telescope and a focusing beam geometry, without significant improvements on the peak intensity at long distances (> 500 m). Collimated beam experiments are discussed here.

Highest laser intensities at long distances were found only when the redder spectral components of the pulse were initially retarded from the bluer components (large negative chirp). For a 200-mJ pulse with a chirp set at or close to its minimum, strong ionization of air was observed over a distance of up to 100 m, starting after a few meters of propagation in air. The beam emerging from the ionization region had a large fraction of its energy converted into a white continuum extending from the ultraviolet to the infrared. The beam also had a significant divergence of the order of 1 mrad, such that the beam intensity rapidly decreased at long distances $d > 500$ m. On the other hand, a strong negatively chirped pulse prevented early filamentation, yet could deliver high intensity at long distances, because of pulse compression due to the group-velocity dispersion of air [1, 26]. The polarization of the laser beam was measured step by step along the propagation axis and remained linear.

Figure 1a and b show single-shot exposures on calibrated photographic plates recorded at 630 and 1010 m. The initial pulse duration was 9.5 ps with negative chirp. The millimeter-size high-intensity spots were rather reproducible from shot-to-shot except for small fluctuations in the transverse position, presumably due to air turbulence, and tended to align along the periphery of a circle approximately equal to that of the initial beam dimension, as can be seen from the image of successive laser shots recorded at 830 m (Fig. 1c–f). Similar

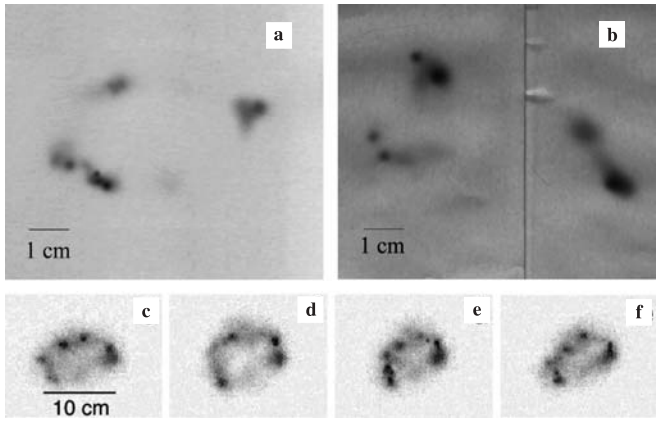

FIGURE 1 Transverse flux recorded by photographic plates. The initial pulse duration was 9.5 ps with negative chirp. **a** 630 m, **b** 1010 m, **c–f** laser shots taken at 0.1-s interval. The image from a diffusor is recorded from a CCD camera at a distance of 830 m

results were obtained with pulse durations ranging between 3 and 10 ps, up to our longest path of 2350 m. More than 80% of the initial pulse energy was still present at a distance of 1 km. Inspection of photographs taken with a smaller contrast showed that most of the laser energy is distributed unevenly between the light channels, with connecting paths between them. We scanned step by step the propagation distances from 0 to 2350 m by our three methods to measure air ionization. Except for a few sporadic events, we were unable to detect ionization signals for large negative chirps (input durations (FWHM) $\tau_p \geq 6$ ps). By decreasing the input duration, ionization could be detected occasionally at some specific propagation distances in the range of large chirps (1.2 ps $\leq \tau_p < 6$ ps). For smaller negative chirps, more intense ionization signals could readily be observed over distances up to 100 m, which corresponds to the classical filamentation regime [7]. From a comparison of the darkening of the photographic plates with that obtained with well-characterized laboratory filaments, we estimated that the peak intensity in the millimeter-size light channels observed up to 2 km is at most 10^{11} W/cm^2, insufficient to induce multiphoton ionization of air molecules.

We have calculated the long-range beam propagation in air using our code, which was modified to properly take into account the realistic beam profile. To our knowledge, genuine three-dimensional simulations of multifilamentation have been performed only twice [16, 19]. Our newly developed $3+1$-dimensional numerical code relies on an extended paraxial model which describes the propagation along the z axis of the slowly varying envelope $\boldsymbol{E}(x, y, z, t)$ of the linearly polarized laser pulse, according to the nonlinear envelope equation [15, 27, 28]. The equation accounts for the following effects. (i) Diffraction. (ii) Group-velocity dispersion and higher-order dispersive terms (exactly computed in Fourier space by means of a Sellmeier dispersion relation for the linear index). (iii) The optical Kerr effect with an instantaneous (electronic) and a delayed component due to stimulated molecular Raman scattering. (iv) Plasma absorption and defocusing. (v) Energy absorption due to photo-ionization. (vi) Deviations from the slowly varying envelope approximation due to space–time focusing and self-steepening of the pulse. Since the measured polarization of the beam remains linear,

the effect of cross-phase modulation is not taken into account, in contrast to [28]. At the same time, the generation of the plasma by an optical field and avalanche ionization is described by the evolution equation for the electron density. The photo-ionization rate is computed from the full Keldysh formulation [29] with a recently determined pre-exponential factor [30].

The measured input-beam profile in the form of a data table was adopted as an initial condition. Negative chirps corresponding to an input duration from its minimum $\tau_p = 120$ fs (without chirp) up to 3 ps were considered, which covers both the small and large negative chirp regimes. We present generic results in the range of negative chirps with 0.5 ps $\leq \tau_p \leq$ 3 ps. The beam energy was 150 mJ. The results for the fluence distribution $F(x, y, z) \equiv \int_{-\infty}^{+\infty} |\boldsymbol{E}(x, y, z, t)|^2 \, dt$, after a propagation distance of 50 m, are compared in Fig. 2 to the measurements. Figure 2 shows several hot spots resulting from the amplification of the inhomogeneities in the input beam. During the self-focusing, the flat-top beam produces rings still visible in the figure. The hot spots develop on these rings that store the main part of the beam energy. In agreement with the experimental results, a significant part of the energy is found unevenly distributed between the light channels. The overall beam-intensity distribution as well as the hot-spot positions and sizes are rather well reproduced. Slight discrepancies between experiments and simulations appear in the azimuthal symmetry. Shot-to-shot fluctuations produce slightly different input beams that generate similar but not rigorously identical patterns after propagating over 50 m. The effect of air turbulence might also induce these differences without destroying the global organization of the light channels. Beyond 60 m, the intensity in the spots falls below 10^{12} W/cm^2. No ionization is detectable after 100 m. These numerical results show that the nonlinear envelope equation satisfactorily describes the experiments even for $P \gg P_{cr}$.

In order to obtain a better insight into the mechanism preventing long-range beam collapse, we have performed simulations assuming a super-Gaussian beam profile that mimics our diaphragmed beam $\boldsymbol{E}(x, y, z = 0, t) \propto \exp[-(x^2 + y^2)^3/w_0^6]$, with a transverse waist $w_0 = 17$ mm, upon which irregularities in the form of different orders of perturbation are added.

First, radially symmetric, super-Gaussian unperturbed input beams remain symmetric during the propagation. As in 2 + 1-dimensional simulations, spatial rings are formed that fuse into one central filament but the rings do not break up into smaller spots. Peak intensities are sufficient to ionize air and the classical filamentation model is recovered, including saturation of self-focusing by a plasma density with peaks around 10^{16} cm^{-3}. Then, we have studied numerically the multifilamentation process occurring from perturbed input beams. Azimuthal perturbations in the form of a mode with a specific order were added to symmetric super-Gaussian input beams. Gaussian input pulses with decreasing negative chirps (pulse durations from 120 fs to 3 ps) were used. The perturbation contains 1% of the energy of the input pulses. The pertubations are amplified preferentially on the ring that develops in the self-focusing stage, leading to its break up into several spots.

Generic results are shown in Fig. 3 for $\tau_p = 1.5$ ps (Fig. 3a and b) and 0.5 ps (Fig. 3c and d) and perturbations in the form of an azimuthal mode of orders nine (Fig. 3a) and ten (Fig. 3c and d). Figure 3a shows isosurfaces of the fluence distribution over a distance of 300 m. A very regular multifilamentation pattern with well-organized light channels is obtained on the ring formed in the first stage. Nine light channels propagate over several tens of meters. The diameters are nearly constant in the millimeter range. The channels are located on

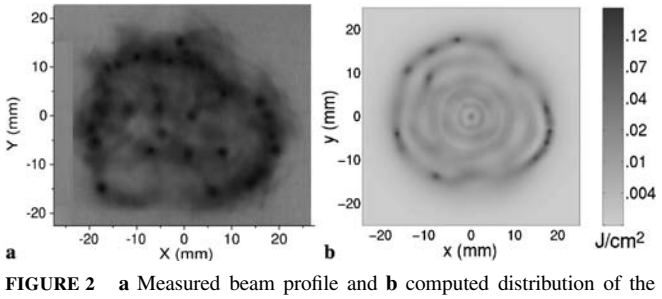

FIGURE 2 **a** Measured beam profile and **b** computed distribution of the fluence at 50 m for $\tau_p = 1.5$ ps

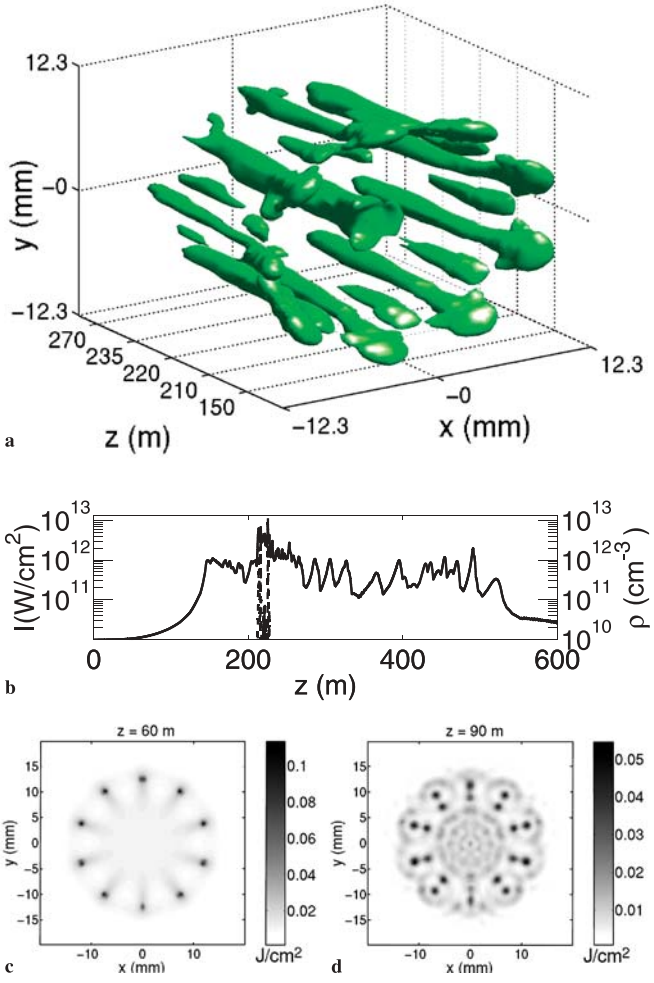

FIGURE 3 **a** Isosurface of the fluence distribution for 0.03 J/cm^2. **b** Maximum intensity (*continuous curve, left-hand axis*) and electron density (*dashed curve, right-hand axis*) as a function of the propagation distance for $\tau_p = 1.5$ ps with negative chirp. **c** and **d** Fluence distributions computed with $\tau_p = 0.5$ ps at **c** $z = 60$ m and **d** $z = 90$ m

a ring slightly smaller than the input-beam radius and regularly spaced like the maximum intensities in the input beam. The pulse duration in the light channels is found to be about 100 fs before a splitting into several subpulses occurs. The same phenomenon is recovered over larger distances from simulations with larger negative chirps.

It is also a generic result that the number of light channels initially follows the order of azimuthal perturbations. When higher-order azimuthal modes are excited, a pattern with a larger number of spots is eventually obtained. Each light channel is well separated and seems to evolve independently from its neighbors. This reflects a competition between the light channels for the surrounding energy. In this respect, the model of the energy reservoir proposed by Mlejnek et al. [16] fully applies except that, in our case, multiphoton ionization does not play a dominant role. Figure 3b shows that the maximum intensity (solid curve, left-hand axis) in the light channels does not exceed a few $10^{12}\,\mathrm{W/cm^2}$. The first stage up to 150 m corresponds to the formation of the light channels under the modulational instability due to the Kerr self-focusing [31]. In the most intense part of the light channels around 210 m, tenuous localized plasma channels of density around a few $10^{12}\,\mathrm{cm^{-3}}$ are triggered (dashed curve, right-hand axis). When the duration of the input pulse is increased, the maximum electron density keeps the same level over a few meters but these localized plasmas are located at increasing distances on the propagation axis. Ionization therefore does not saturate self-focusing as in classical femtosecond filamentation. Yet, it acts locally as a necessary regularizing process during the propagation of the light channels. Simulations performed by unplugging ionization indeed show that the maximum intensity follows the solid curve in Fig. 3b except for slightly higher peaks in the region of the plasma and an eventual catastrophic collapse before $z = 210$ m. Figure 3c and d show the evolution of the fluence distribution from 60 to 90 m for $\tau_p = 0.5$ ps. A break up of each filament into two smaller light channels occurs around 60 m. Beyond 90 m, each pair of these co-propagating channels merge (pattern similar to Fig. 3c). This shows nicely how daughter channels are formed along light tracks due to interference in the coherent beam. In this sense, both interference and the nonlinear Kerr effect act to redirect the energy from parent to daughter light channels.

In conclusion, long-range-propagation studies of intense laser pulses in the atmosphere reveal the existence of stable non-ionizing channels extending over km distance. For the first time, their spatial and temporal dynamics is compared to genuine $3+1$-dimensional numerical simulations. Well-ordered filamentation patterns exhibit a beautiful organization of the spots on concentric rings, which reproduce the patterns obtained in the experiments. Such results are described by using the same nonlinear propagation equation that describes the filamentation at low input power, without the necessity to add a new physical mechanism to limit the growth of laser intensity. Model simulations uncover the complexity of the nonlinear system, where initial conditions play a crucial role for the later evolution of the system.

ACKNOWLEDGEMENTS This work was made within the framework of the joint French–German teramobile project funded by the CNRS and the DFG. A.M. acknowledges support from the Humboldt Foundation. We also acknowledge partial support from NATO program TG31.

REFERENCES

1 P. Rairoux, H. Schillinger, S. Neirdeimer, M. Rodriguez, F. Ronneberger, R. Sauerbrey, B. Stein, D. Waite, C. Wedekind, H. Wille, L. Wöste, C. Ziener: Appl. Phys. B **71**, 573 (2000)
2 L. Wöste, C. Wedekind, H. Wille, P. Rairoux, B. Stein, S. Nikolov, C. Werner, S. Neirdeimer, F. Ronneberger, H. Schilinger, R. Sauerbrey: Laser Optoelectron. **29**, 51 (1997)
3 J. Kasparian, M. Rodriguez, G. Méjean, J. Yu, E. Salmon, H. Wille, R. Bourayou, S. Frey, Y.-B. André, A. Mysyrowicz, R. Sauerbrey, J.-P. Wolf, L. Wöste: Science **301**, 61 (2003)
4 F. Vidal, D. Comtois, C.-Y. Chien, A. Desparois, B. La Fontaine, T.W. Johnston, J.-C. Kieffer, H.P. Mercure, F.A. Rizk: IEEE Trans. Plasma Sci. **28**, 418 (2000)
5 X.M. Zhao, J.-C. Diels, C.Y. Wang, J.M. Elizondo: IEEE J. Quantum Electron. **31**, 599 (1995)
6 Y. Silberberg: Opt. Lett. **15**, 1282 (1990)
7 E.T.J. Nibbering, P.F. Curley, G. Grillon, B.S. Prade, M.A. Franco, F. Salin, A. Mysyrowicz: Opt. Lett. **21**, 62 (1996)
8 O.G. Kosareva, V.P. Kandidov, A. Brodeur, C.Y. Chien, S.L. Chin: Opt. Lett. **22**, 1332 (1997)
9 N. Aközbek, M. Scalora, C.M. Bowden, S.L. Chin: Opt. Commun. **191**, 353 (2001)
10 S. Tzortzakis, G. Méchain, G. Palatano, Y.-B. André, M. Franco, B. Prade, A. Mysyrowicz: Opt. Lett. **27**, 1944 (2002)
11 C.-C. Cheng, E.M. Wright, J.V. Moloney: Phys. Rev. Lett. **87**, 213 001 (2001)
12 V.S. Letokhov: in *Proc. XXII Solvay Conf. Physics* (World Scientific 2001)
13 H.R. Lange, A. Chiron, J.-F. Ripoche, A. Mysyrowicz, P. Breger, P. Agostini: Phys. Rev. Lett. **81**, 1611 (1998)
14 A. Braun, G. Korn, X. Liu, D. Du, J. Squier, G. Mourou: Opt. Lett. **20**, 73 (1995)
15 A. Couairon, S. Tzortzakis, L. Bergé, M. Franco, B. Prade, A. Mysyrowicz: J. Opt. Soc. Am. B **19**, 1117 (2002)
16 M. Mlejnek, M. Kolesik, J.V. Moloney, E.M. Wright: Phys. Rev. Lett. **83**, 2938 (1999)
17 A. Iwasaki, N. Aközbek, B. Ferland, Q. Luo, G. Roy, C.M. Bowden, S.L. Chin: Appl. Phys. B **76**, 231 (2003)
18 B. La Fontaine, F. Vidal, Z. Jiang, C.Y. Chien, D. Comtois, A. Desparois, T.W. Johnston, J.-C. Kieffer, H. Pépin: Phys. Plasmas **6**, 1615 (1999)
19 S.L. Chin, A. Talebpour, J. Yang, S. Petit, V.P. Kandidov, O.G. Kosareva, M.P. Tamarov: Appl. Phys. B **74**, 67 (2002); V.P. Kandidov, O.G. Kosareva, M.P. Tamarov, A. Brodeur, S.L. Chin: Quantum Electron. **29**, 911 (1999)
20 Millimeter-sized filaments at a distance of 200 m have been reported by several groups [18, 19]
21 H. Wille, M. Rodriguez, J. Kasparian, D. Mondelain, J. Yu, A. Mysyrowicz, R. Sauerbrey, J.-P. Wolf, L. Wöste: Eur. Phys. J.: Appl. Phys. **20**, 183 (2002)
22 S. Tzortzakis, B. Lamouroux, A. Chiron, M. Franco, B. Prade, A. Mysyrowicz, S.D. Moustaizis: Phys. Rev. E **60**, R3505 (1999)
23 H.D. Ladouceur, A.P. Baronavski, D. Lohrmann, P.W. Grounds, P.G. Girardi: Opt. Commun. **189**, 107 (2001)
24 H. Schillinger, R. Sauerbrey: Appl. Phys. B **68**, 753 (1999)
25 A. Talebpour, S. Petit, S.L. Chin: Opt. Commun. **171**, 285 (1999)
26 P. Sprangle, J.R. Peñano, B. Hafizi: Phys. Rev. E **66**, 046 418 (2002)
27 T. Brabec, F. Krausz: Phys. Rev. Lett. **78**, 3282 (1997)
28 A. Couairon, G. Méchain, S. Tzortzakis, M. Franco, B. Lamouroux, B. Prade, A. Mysyrowicz: Opt. Commun. **225**, 177 (2003)
29 L.V. Keldysh: ZhETF **47**, 1945 (1964); Sov. Phys. JETP **20**, 1307 (1965)
30 K. Mishima, M. Hayashi, J. Yi, S.H. Lin, H.L. Selzle, E.W. Schlag: Phys. Rev. A **66**, 033 401 (2002)
31 V.I. Bespalov, V.I. Talanov: JETP Lett. **3**, 307 (1966)